Molecular Therapy
Nucleic Acids
Original Article

Preclinical evaluation of WVE-004, aninvestigational stereopure oligonucleotide forthe treatment of *C9orf72*-associated ALS or FTD

Yuanjing Liu,[1] Amy Andreucci,[1] Naoki Iwamoto,[1] Yuan Yin,[1] Hailin Yang,[1] Fangjun Liu,[1] Alexey Bulychev,[1] Xiao Shelley Hu,[1] Xuena Lin,[1] Sarah Lamore,[1] Saurabh Patil,[1] Susovan Mohapatra,[1] Erin Purcell-Estabrook,[1] Kristin Taborn,[1] Elena Dale,[1] and Chandra Vargeese[1]

[1]Wave Life Sciences, 733 Concord Avenue, Cambridge, MA 02138, USA

A large hexanucleotide (G_4C_2) repeat expansion in the first intronic region of *C9orf72* is the most common genetic cause of amyotrophic lateral sclerosis (ALS) and frontotemporal dementia (FTD). Several mechanisms have been proposed to explain how the repeat expansion drives disease, and we hypothesize that a variant-selective approach, in which transcripts affected by the repeat expansion are preferentially decreased, has the potential to address most of them. We report a stereopure antisense oligonucleotide, WVE-004, that executes this variant-selective mechanism of action. WVE-004 dose-dependently and selectively reduces repeat-containing transcripts in patient-derived motor neurons carrying a *C9orf72*-repeat expansion, as well as in the spinal cord and cortex of C9 BAC transgenic mice. In mice, selective transcript knockdown was accompanied by substantial decreases in dipeptide-repeat proteins, which are pathological biomarkers associated with the repeat expansion, and by preservation of healthy C9orf72 protein expression. These *in vivo* effects were durable, persisting for at least 6 months. These data support the advancement of WVE-004 as an investigational stereopure antisense oligonucleotide targeting C9orf72 for the treatment of *C9orf72*-associated ALS or FTD.

INTRODUCTION

The most common known genetic cause of inherited and sporadic forms of both amyotrophic lateral sclerosis (ALS) and frontotemporal dementia (FTD) is a large hexanucleotide GGGGCC (G_4C_2) repeat expansion in the first intronic region of *C9orf72*.[1–3] Despite being distinct disorders, studies have found that ~20%–50% of patients have both *C9orf72*-associated ALS and FTD.[1,4–6] Together, the overlap in genetics, pathology, and clinical presentation has led to the idea that these diseases are manifestations of a clinical spectrum, referred to as *C9orf72*-associated ALS or FTD (C9-ALS/FTD).[7–9]

ALS is caused by the degeneration of upper and lower motor neurons. The rapid progression of the disease leads to muscle weakness, paralysis, and eventually death from respiratory failure.[10–12] Roughly 2,000 people in the United States have C9-ALS.[6,8,13–16] The average age of C9-ALS disease onset is 57.9 years, with a mean disease duration of 3.1 years.[17] FTD is a fatal condition characterized by the degeneration of the frontal and temporal cortices. Affected individuals will show personality and behavior changes as well as a gradual impairment of language skills.[10,12,18] C9-FTD affects approximately 10,000 people in the United States.[3,13,19–22] The average age of disease onset is 58.2 years, with a disease duration of 6.4 years.[20] C9-ALS/FTD is associated with severe cognitive and behavioral impairments, and patients typically have schizophrenic-like symptoms such as hallucinations, delusions, and disordered thinking.[6,23,24] These patients also have a lower age of onset paired with reduced survival time compared with patients with ALS or FTD without the *C9orf72* expansions.[6] Two approved therapies for ALS are available in the United States; however, these treatments only slow disease progression in certain patients.[14,25,26] Currently, there are no approved disease-modifying therapies for FTD. Thus, there is a significant unmet need for effective therapies for patients with ALS and FTD, including those with *C9orf72*-repeat expansions.

C9orf72 protein is involved in a variety of pathways within the central nervous system (CNS). In neurons, C9orf72 is believed to be involved in membrane trafficking, autophagy, phagocytosis, and endocytosis.[27–29] *C9orf72* encodes three transcripts: variant 1 (V1), V2, and V3.[18,30] V2 expression is higher than V1 and V3 in the CNS.[18] The G_4C_2-repeat region is located within the promoter region of V2, and expansion of this region can impact V2 expression but does not modify the V2 pre-mRNA product.[18,30] In contrast, the repeat region is located within intron 1 of V1 and V3, and the repeat expansion leads to production of modified sense and antisense transcripts that can form nuclear RNA foci and encode dipeptide protein repeats (DPRs).[10,30,31]

Received 12 August 2021; accepted 15 April 2022;
https://doi.org/10.1016/j.omtn.2022.04.007.

Correspondence: Chandra Vargeese, PhD, Wave Life Sciences, 733 Concord Avenue, Cambridge, MA 02138, USA.
E-mail: cvargeese@wavelifesci.com

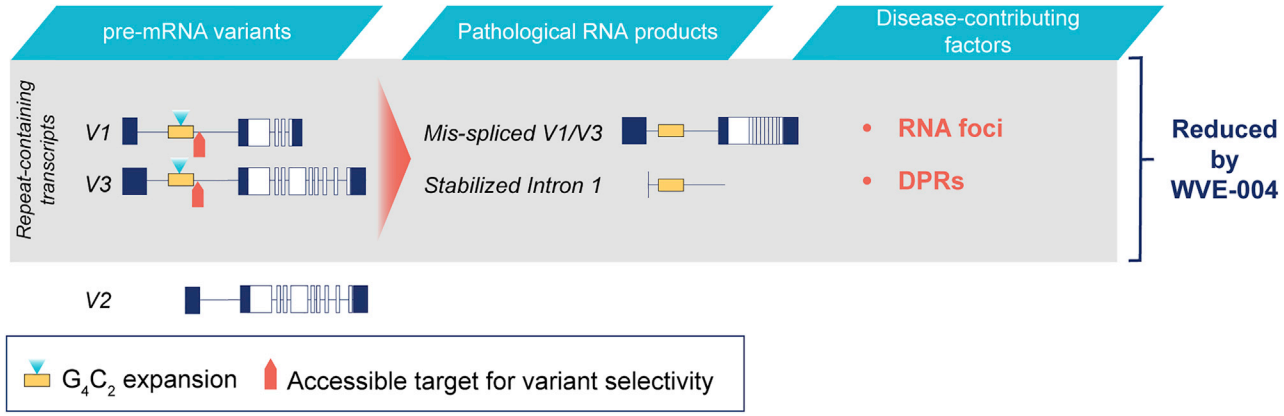

Figure 1. Variant-selective targeting strategy preserves healthy C9orf72 protein

WVE-004 is designed to selectively silence the pre-mRNA repeat-containing variants V1 and V3, which ultimately lead to DPRs and RNA foci, while sparing the V2 transcript, which is the main contributor to C9orf72 protein expression. This selectivity is achieved by directing WVE-004 to a sequence that is only accessible in V1 and V3 transcripts.[7]. DPR, dipeptide repeat protein; V, variant.

Several mechanisms have been proposed to explain how the repeat expansion in *C9orf72* leads to C9-ALS/FTD.[18,29,32] The repeat expansion can decrease expression of C9orf72 protein, resulting in a partial loss of function, which is referred to as haploinsufficiency.[33] Decreasing *C9orf72* expression in mice increases microglial activation, and knocking it out leads to a pro-inflammatory state.[34,35] This inflammation of the CNS could lead to toxicity in neurons and neurodegeneration.[36] Bidirectional transcription of expanded repeats resulting in the production of sense and antisense RNAs containing the repeats may also contribute to disease.[18,29,32] These RNAs may recruit and sequester RNA-binding proteins, forming RNA foci. This, in turn, may lead to toxicity, as the sequestered RNA-binding proteins are no longer able to carry out their normal functions, such as participating in splicing, translational regulation, and RNA transport and degradation.[18,29,32] Finally, both sense and antisense repeat RNAs can be translated via repeat-associated non-ATG (RAN) translation to encode toxic DPRs, such as poly-glycine-proline (poly-GP).[18,32,37–39] DPRs can form aggregates within the nucleoli, causing a stress response in cells and the formation of stress granules, leading to neurotoxicity.[32,40,41] These mechanisms are probably not mutually exclusive, as a few recent publications examining motor neurons and transgenic mice showed a synergized effect of C9orf72 reduction and DPR toxicity.[35,37,42] Because both a loss and gain of function associated with *C9orf72* expansion likely contribute to the disease, an important goal of therapeutics targeting *C9orf72* is to reduce the expression of pathological transcripts while maintaining the expression of healthy C9orf72 protein.

Previous studies have shown that antisense oligonucleotides can lead to the selective reduction of C9orf72-repeat-containing transcripts as well as DPR proteins, which are believed to drive disease pathology.[7,38,43] Treating transgenic mice that express an expanded, albeit truncated, version of the human *C9orf72* gene with one of these oligonucleotides improved behavioral defects.[44] This suggests that selective knockdown of repeat-containing transcripts in affected regions of the brain may be a promising therapeutic approach for the treatment of C9-ALS/FTD.

We previously reported on a targeting sequence, called splice site 1b (SS1b), that is common to all C9orf72 transcripts but enables preferential knockdown of repeat-containing transcripts *in vitro* and *in vivo* with a stereopure antisense oligonucleotide.[7] Subsequent data have shown that the potency, CNS delivery, and duration of activity of stereopure antisense oligonucleotides can be improved by introducing phosphoryl guanidine-containing backbone linkages (phosphoryl guanidine [PN] chemistry) into their backbone.[45] This modification, like the more-familiar phosphorothioate (PS) modification, replaces the phosphodiester (PO) bond with a nitrogen-containing moiety in the oligonucleotide backbone, creating a chiral configuration. With PS modification, the oxygen is replaced by sulfur; with PN modification, the oxygen is replaced by a phosphoryl-guanidine moiety. Leveraging these discoveries, we have developed the investigational stereopure antisense oligonucleotide WVE-004 as a potential disease-modifying therapy for C9-ALS/FTD. WVE-004 was designed to selectively deplete V1 and V3 transcripts while sparing V2 transcripts and preserving C9orf72 protein (Figure 1). Here, we present *in vitro* and *in vivo* experiments in pre-clinical models evaluating the effects of WVE-004 on C9orf72 repeat-containing transcripts, DPR proteins, and total C9orf72 protein levels.

RESULTS

WVE-004 selectively and dose dependently decreases V3 *in vitro*

We treated ALS motor neurons derived from induced pluripotent stem cells (iPSCs) from a patient carrying a *C9orf72*-repeat expansion with WVE-004 or a non-targeting control oligonucleotide (NTC) at varying levels up to a 10 μM concentration under gymnotic (i.e., free-uptake conditions) and assessed C9orf72 transcript knockdown for all variants as well as for V3 alone. V3 transcripts served as an indicator of the level of repeat-containing transcripts, as V3 is the most highly expressed of these transcripts.[8]

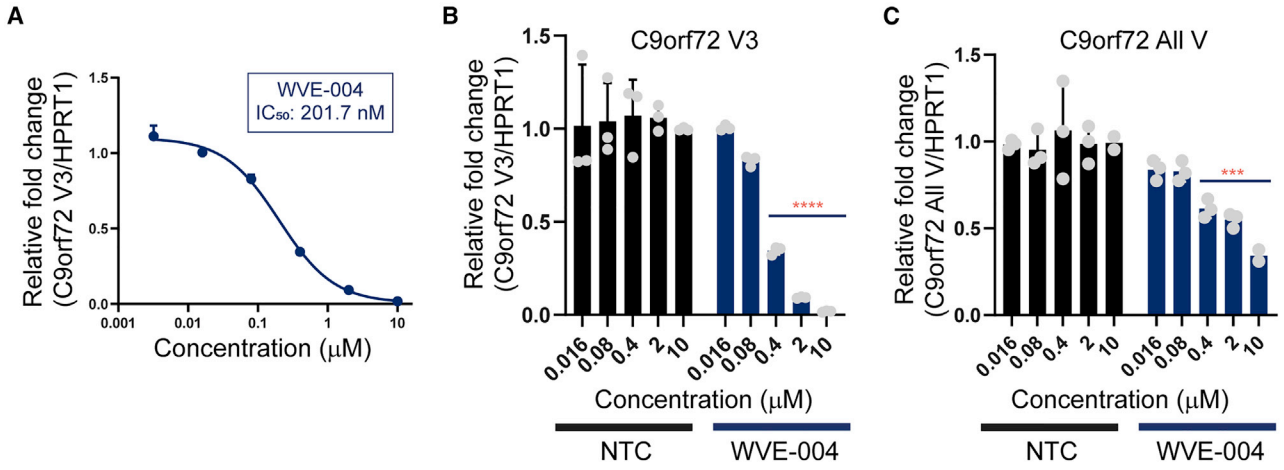

Figure 2. Potent and selective knockdown of repeat-containing transcripts *in vitro* with WVE-004

We treated *C9orf72* patient-derived motor neurons with WVE-004 or an NTC at varying levels up to a 10 μM concentration. (A) The dose-response curve of C9orf72 V3 normalized to *HPRT1* mRNA at varying levels up to a 10 μM concentration (n = 3). Data are shown as mean ± SD. (B and C) The relative fold change of C9orf72 V3 (B) or all variants including V3 (all V) (C) with respect to *HPRT1*. Data are show as a scatterplot with mean ± SD (V3, n = 3; all V, n = 2–3; ***p ≤ 0.001, ****p ≤ 0.0001 versus NTC). IC_{50}, half-maximal inhibitory concentration; NTC, nontargeting control; V, variant.

WVE-004 knocked down V3 transcripts in a dose-dependent manner, demonstrating a 201.7 nM half-maximal inhibitory concentration (IC_{50}) (Figure 2A). Compared with NTC, WVE-004 potently and selectively reduced V3 transcripts with a mean knockdown of 98.1% for V3 at 10 μM (Figure 2B). WVE-004 showed lower potency toward all transcriptional variants, which include V3, with a mean knockdown of 65.7% at 10 μM (Figure 2C), indicating a preferential knockdown of repeat-containing transcripts. Together, these data demonstrate that WVE-004 leads to dose-dependent, potent, and selective decrease of C9orf72 repeat-containing transcripts *in vitro* in patient-derived motor neurons under free-uptake conditions.

WVE-004 is not cytotoxic or pro-inflammatory

Before testing WVE-004 *in vivo*, we evaluated its cellular toxicity and pro-inflammatory activity. For these experiments, we benchmarked WVE-004 against ODN 2216, a known Toll-like receptor 9 (TLR9) agonist that can activate secretion of some pro-inflammatory cytokines in peripheral blood mononuclear cells (PBMCs).[44] We performed cellular cytotoxicity assays in PBMCs, which showed that WVE-004 did not induce cytotoxicity (≤80% viability) at concentrations up to 30 μM (Figure S1).To evaluate inflammatory potential, we quantified PBMC secretion of cytokines in response to WVE-004 or ODN 2216 (Figure S1). Cytokine secretion was also benchmarked against phosphate-buffered saline (PBS), which served as a negative control. For multiple cytokines, secretion upon treatment with WVE-004 tracked well with responses to PBS. For others, the highest concentration of WVE-004 (30 μM) led to more cytokine secretion than PBS but far less than ODN 2216. Overall, these data indicate that WVE-004 does not induce cytotoxicity and that it induced relatively low cytokine production compared with the positive control *in vitro* at the concentrations tested in this assay. WVE-004's impact on PBMC cytokine secretion is consistent with our prior report that PN-modified oligonucleotides are not pro-inflammatory and may be less inflammatory than a PS-modified counterpart,[45] which may be critical if the *C9orf72*-repeat expansion leads to a pro-inflammatory state.[34,35]

WVE-004 distributes to targeted brain regions *in vivo*

To determine whether WVE-004 distributes to CNS tissues affected in C9-ALS/FTD *in vivo*, we administered PBS or 100 μg of oligonucleotide (50 μg on days 0 and 7) by intracerebroventricular (i.c.v.) injection to *C9orf72* BAC transgenic (C9 BAC) mice containing the full human *C9orf72* gene with a repeat expansion[46] and processed tissue 8 weeks later for visualization by *in situ* hybridization. We detected WVE-004 throughout the spinal cord, including in motor neurons of the anterior horn, and in the cortex, including in neurons in the deep layers of the neocortex (Figure 3). Broad distribution of WVE-004 was seen in other brain and spinal cord regions as well, including the dentate gyrus and cornu ammonis regions of the hippocampus, the Purkinje and granular layers of the cerebellum, the brain stem, and the posterior horn of the spinal cord (Figure S2). WVE-004 was detectable by this method in the spinal cord until at least 24 weeks after the first injection (Figure S3). These data show that WVE-004 reaches tissues in C9 BAC mice that are most profoundly affected in C9-ALS/FTD.

WVE-004 selectively and dose-dependently decreases V3 *in vivo*

Multiple mouse lines have been generated to model C9-ALS/FTD.[46–49] To characterize the *in vivo* activity of WVE-004, we chose the C9 BAC line[47] because it expresses the full-length, repeat-expansion-containing human *C9orf72* gene and expresses C9orf72 protein, giving us more confidence that it will better recapitulate transcription-dependent and C9orf72-protein-related pathologies associated with disease compared with models expressing a truncated gene. Our prior work in these mice showed that variant-selective stereopure oligonucleotides targeting SS1b lead to the durable depletion of RNA foci and DPRs.[7] To evaluate

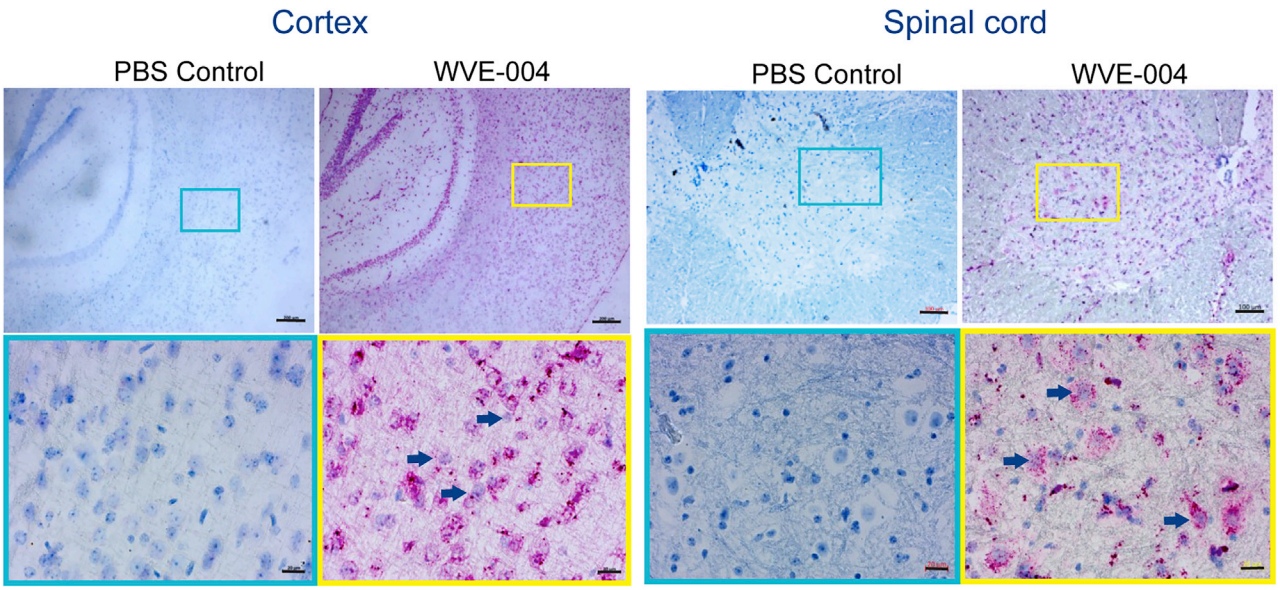

Figure 3. WVE-004 reaches target brain regions *in vivo*

We administered PBS or 50 μg of WVE-004 by i.c.v. injection to C9 BAC mice on days 0 and 7. Representative images from *in situ* hybridization probing for WVE-004 in layer IV of the cortex (left) and anterior horn of the spinal cord (right) in C9 BAC mouse tissues 8 weeks after the first injection. WVE-004 is stained in red (fast red), and nuclei are stained in blue (hematoxylin). Bright-field images in the top row are at 5× magnification, and scale bars are 200 (cortex) and 100 μm (spinal cord). Images in the bottom row are at 40× magnification, and scale bars are 20 μm. Blue arrowheads point to nuclei containing WVE-004. i.c.v., intracerebroventricular; PBS, phosphate-buffered saline.

the activity of WVE-004 *in vivo* in C9 BAC mice, we administered PBS or oligonucleotide by i.c.v. injection at varying doses up to a total dose of 100 μg in mice that were 4–5 months of age, which was 1–2 months after the onset of disease pathologies associated with the *C9orf72*-repeat expansion.[47] Our goal was to minimize the dose needed to achieve both target engagement—a decrease in C9orf72 repeat-containing transcripts—and a pharmacodynamic effect—a decrease in poly-GP DPR protein levels. Poly-GP is a potential biomarker that can be feasibly monitored during clinical trials for therapeutics targeting *C9orf72*-repeat expansions.[39,50,51] Poly-GP is detectable in the cerebrospinal fluid (CSF) of individuals with the *C9orf72*-expansion mutation,[39,50,51] and poly-GP is the only DPR that mirrors expression of both sense and antisense repeat-containing C9orf72 transcripts.[39]

WVE-004 dose-dependently decreased V3 transcripts and poly-GP in spinal cord tissue of C9 BAC mice (Figure 4A). WVE-004 knocked down V3 transcripts by a mean of 58.9% ($p \leq 0.0001$) and 84.2% ($p \leq 0.0001$) at the 30 and 100 μg total dose levels, respectively, compared with PBS. Mean poly-GP levels were reduced by 61.2% ($p \leq 0.01$), 94.7% ($p \leq 0.0001$), and 96.4% ($p \leq 0.0001$) compared with PBS at the 10, 30, and 100 μg total dose levels, respectively. In mouse cortex, WVE-004 knocked down V3 transcripts by a mean of 26.8% ($p \leq 0.01$) and 59.3% ($p \leq 0.0001$) at the 30 and 100 μg dose levels, respectively, compared with PBS. Mean poly-GP levels were reduced by 79.8% ($p \leq 0.001$) at the 100 μg total dose compared with PBS (Figure 4B), and only the 100 μg total dose level achieved statistically significant effects on poly-GP in the cortex. These data demonstrate that WVE-004 has a dose-dependent effect on V3 transcripts and poly-GP in the CNS of C9 BAC mice and that the 100 μg total dose level is sufficient to achieve the desired effects on V3 transcripts and poly-GP in the spinal cord and cortex.

Effects of WVE-004 *in vivo* are durable

We next assessed the duration of response of WVE-004 at the 100 μg total dose level *in vivo* in the same mouse model. We initially evaluated the durability of WVE-004's effects in a 2-month-long experiment. We assessed the effects of WVE-004 on repeat-containing transcripts by evaluating V3. We assessed variant selectivity by evaluating all transcriptional variants and C9orf72 protein, and we assessed pharmacodynamic effect by evaluating poly-GP. In the spinal cord, WVE-004 significantly decreased V3 transcripts at 2, 4, and 8 weeks post-first dose compared with PBS treatment ($p \leq 0.001$). At the same time points, expression of all C9orf72 transcriptional variants, including V3, was also decreased but to lesser extent than V3, indicating that WVE-004 was selective for V3 (Figure 5A). C9orf72 protein levels remained unchanged at 8 weeks compared with PBS-treated animals (Figure S4), which further supports the notion that WVE-004 is selective for repeat-containing variants. Poly-GP levels were decreased to nearly undetectable levels at all time points (Figure 5A). In the cortex, WVE-004 significantly decreased V3 transcripts at all time points evaluated compared with PBS treatment ($p \leq 0.01$), and the magnitude of decrease increased with each subsequent time point. Expression of all C9orf72 transcriptional variants, which were not significantly different relative to PBS treatment, indicated that WVE-004 was selective for repeat-containing transcripts (Figures 5B and S4).

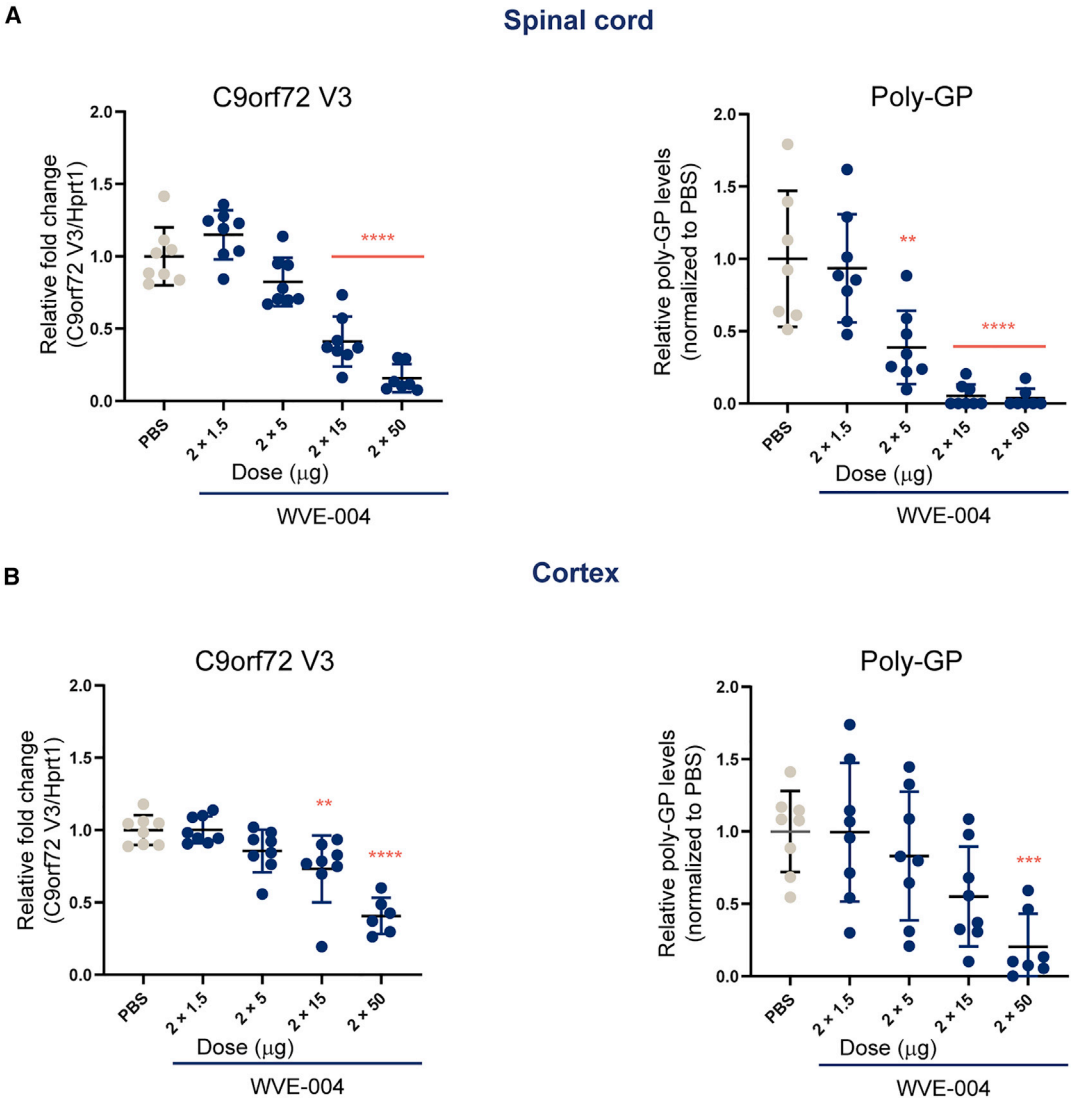

Figure 4. WVE-004 shows dose-dependent knockdown of V3 transcripts and poly-GP in a C9 BAC mouse model

We administered PBS or the indicated dose of WVE-004 by i.c.v. injection to C9 BAC transgenic mice on days 0 and 7. Mice were euthanized 6 weeks after the first administration. (A and B) The relative fold change of human C9orf72 V3 to mouse Hprt1 mRNA (left) and the relative poly-GP levels normalized to PBS (right) are shown in the spinal cord (A) and the cortex (B). Data are shown as a scatterplot with mean ± SD (n = 7–8, **p < 0.01, ***p < 0.001, ****p < 0.0001 versus PBS). p values were calculated via one-way ANOVA, followed by Dunnett's multiple comparison test. ANOVA, analysis of variance; i.c.v., intracerebroventricular; PBS, phosphate-buffered saline; poly-GP, poly-glycine-proline; V, variant.

Poly-GP levels were substantially decreased at all time points compared with PBS-treated animals (Figure 5B). Variation in poly-GP expression in control animals was substantial in this experiment, but the consistent decline observed in WVE-004-treated animals gave us confidence that WVE-004 was driving the decline. Together, these data indicate that a 100 μg total dose of WVE-004 selectively decreases repeat-containing transcripts and the biomarker poly-GP, while preserving the expression of C9orf72 protein in both the spinal cord and cortex of C9 BAC mice. Because the effects of WVE-004 were consistent or still improving at the 2-month time point, we performed a longer experiment, extending it out to 6 months, to determine how long the effects of WVE-004 persist.

Following the same dosing regimen described above, we administered PBS or oligonucleotide to C9 BAC mice, and we assessed the effect on C9orf72 repeat-containing transcripts and poly-GP 4, 12, 18, and 24 weeks after the first injection. In both the spinal cord and cortex, we found a significant effect of WVE-004 treatment on V3 transcripts and poly-GP levels at all time points evaluated. WVE-004 led to a 66%–87% ($p < 0.001$) and 35%–49%

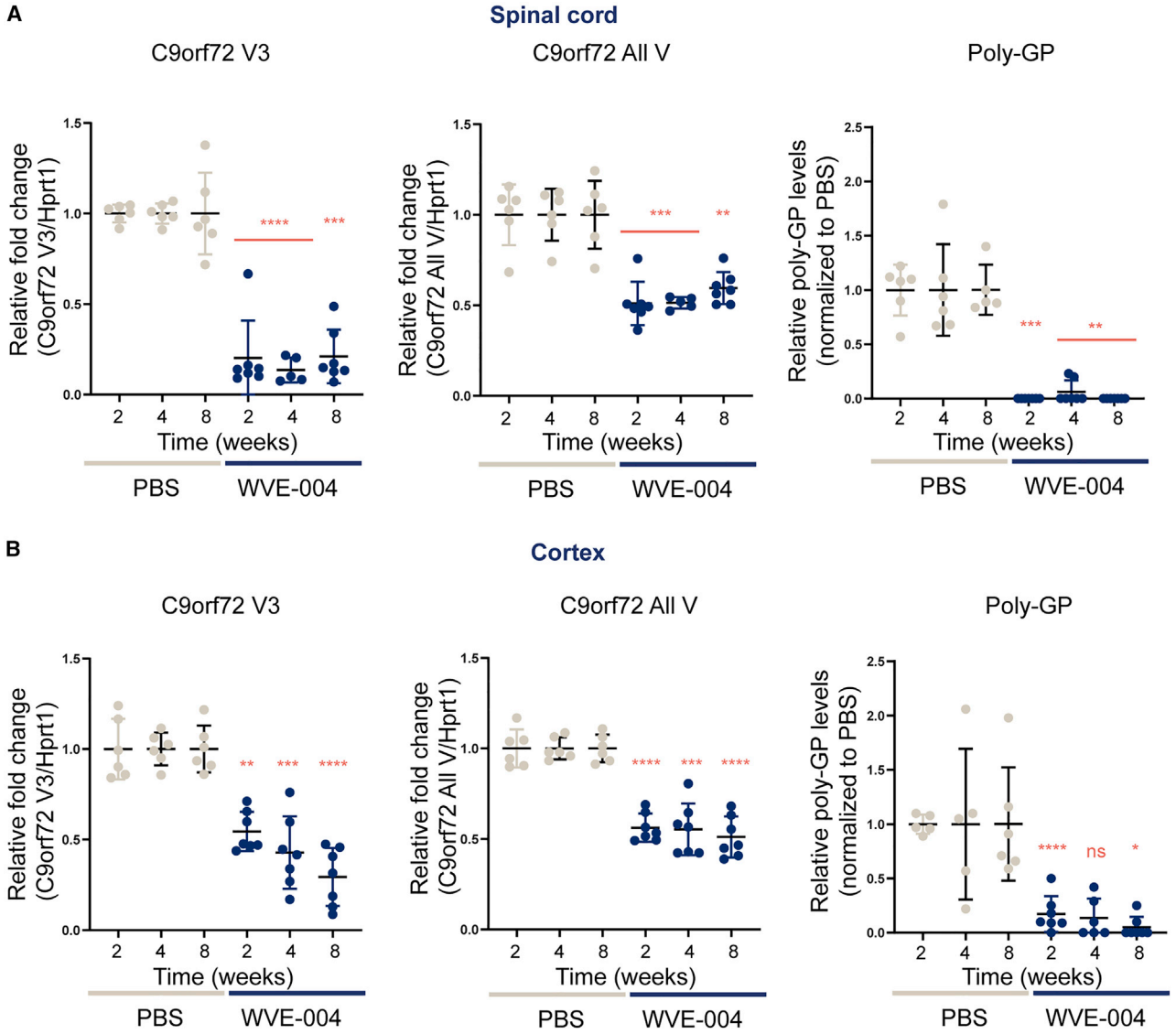

Figure 5. WVE-004 selectively knocks down repeat-containing transcripts and poly-GP for at least 2 months in cortex and spinal cord

We administered PBS or 50 μg WVE-004 by i.c.v. injection to C9 BAC transgenic mice on days 0 and 7. (A) The relative fold change of human C9orf72 V3 to mouse Hprt1 mRNA, all C9orf72 transcriptional variants to mouse Hprt1 mRNA, and the relative poly-GP level (n = 6–7) in the spinal cord are shown at 2, 4, and 8 weeks after the first administration. (B) The relative fold change of the same biomarkers in the cortex (n = 6–7) is shown for the same time points. Data are shown as a scatterplot with mean ± SD (ns, non-significant, *$p < 0.05$, **$p < 0.01$, ***$p < 0.001$, ****$p < 0.0001$ versus PBS). p values were calculated via two-way ANOVA, followed by Sidak's multiple comparison test. ANOVA, analysis of variance; i.c.v., intracerebroventricular; PBS, phosphate-buffered saline; poly-GP, poly-glycine-proline; V, variant.

($p < 0.01$) mean knockdown of V3 transcripts in the spinal cord and cortex, respectively, through 24 weeks after dosing (Figures 6A and 6B). WVE-004 led to a ≥94% ($p < 0.05$) and ≥84% ($p < 0.01$) knockdown of poly-GP in the spinal cord and cortex, respectively, through 24 weeks after dosing (Figures 6A and 6B). These data indicate that WVE-004 has a durable impact on both V3 transcripts and poly-GP in the CNS of C9 BAC mice. We also tested whether C9orf72 protein levels were affected by WVE-004 treatment. Mice treated with 100 μg of WVE-004 showed comparable levels of C9orf72 protein to mice treated with PBS 24 weeks after dosing (Figures 6A and 6B). In combination with the target engagement and pharmacodynamic data described above, these data illustrate that WVE-004 executes the desired variant-selective mechanism of action and has a remarkably durable impact in C9 BAC mice.

Effects of WVE-004 *in vivo* persist at low levels of tissue exposure

To further analyze the data from the *in vivo* studies, we evaluated the relationship between WVE-004 tissue-exposure levels in both spinal

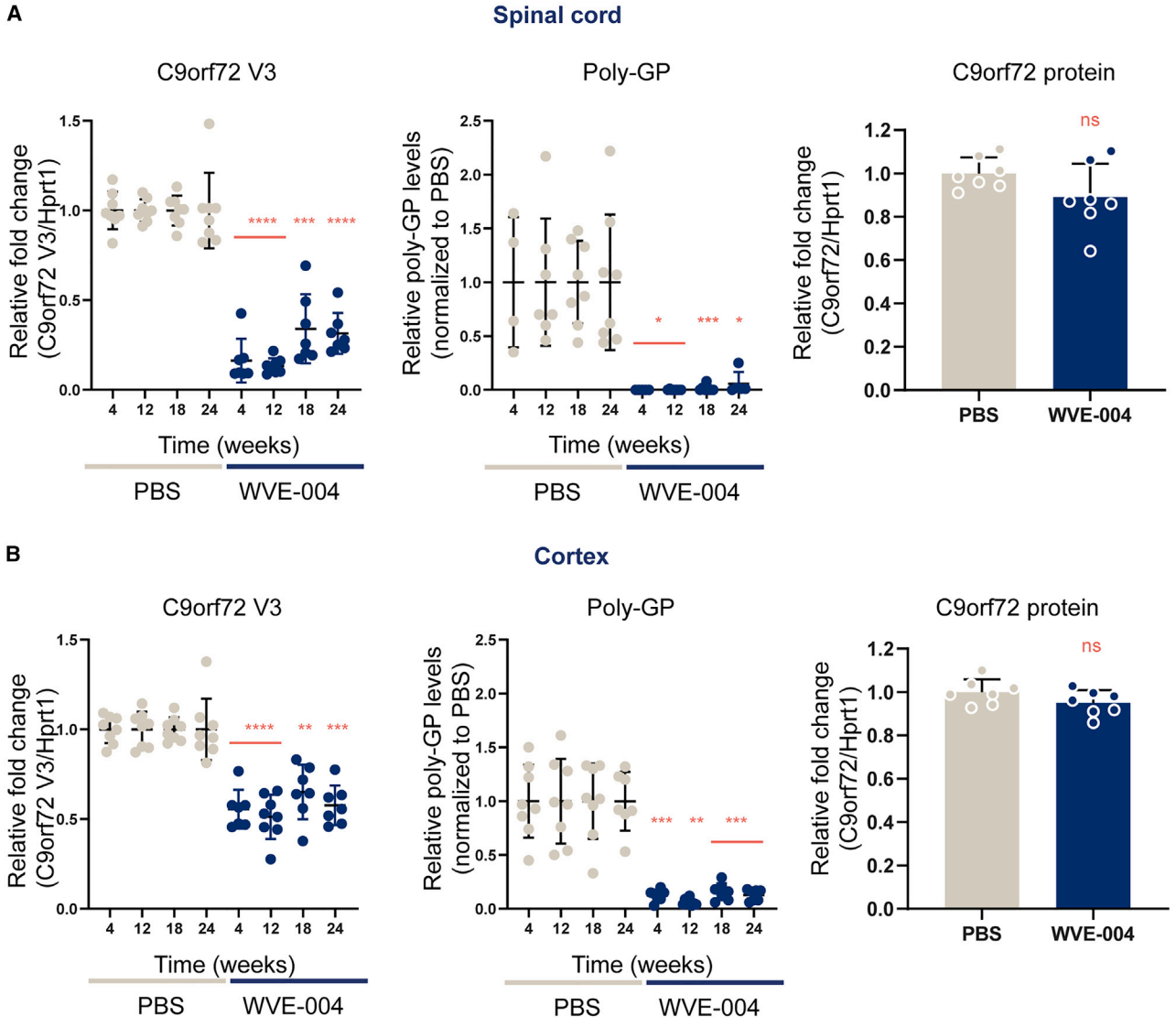

Figure 6. WVE-004 shows durable knockdown of repeat-containing transcripts and poly-GP while preserving C9orf72 protein expression *in vivo* up to 24 weeks after dosing

We administered PBS or 50 μg WVE-004 by i.c.v. injection to C9 BAC transgenic mice on days 0 and 7. (A) The relative fold change of human C9orf72 V3 to mouse Hprt1 mRNA, the relative poly-GP level, and the relative C9orf72 protein level in the spinal cord are shown at 4, 12, 18, and 24 weeks after the first administration (n = 4–8). (B) The relative fold change of the same biomarkers is shown for the cortex (n = 4–8) for the same time points. Data are shown as a scatterplot with mean ± SD (ns, non-significant, **p < 0.01, ***p < 0.001, ****p < 0.0001 versus PBS). p values were calculated via two-way ANOVA, followed by Sidak's multiple comparison test. ANOVA, analysis of variance; i.c.v., intracerebroventricular; PBS, phosphate-buffered saline; poly-GP, poly-glycine-proline; V, variant.

cord and cortical tissue (Figure S5) and the observed pharmacodynamic effects (data shown in Figures 4, 5, and 6). This analysis showed that the concentration of WVE-004 in spinal cord and cortex increased with dose, and the increase in tissue concentration was correlated with observed decreases in V3 transcripts and poly-GP levels (Figure 7A). The analysis allowed us to calculate *in vivo* IC_{50} values for WVE-004 in spinal cord (IC_{50} = 0.45 μg/g) and cortex (IC_{50} = 0.52 μg/g), which confirm that WVE-004 is a potent silencer of V3 expression.

We used these same datasets to better understand the kinetics of WVE-004. The concentrations of WVE-004 were highest in the spinal cord through the 8-week time point and steadily declined at later time points (Figure 7B). WVE-004 concentrations increased in the cortex up to week 6, remaining at peak levels through week 8, and declined rapidly between 8 and 12 weeks (Figure 7B). These kinetic data allowed us to estimate the half-life ($t_{1/2}$) for WVE-004 in spinal cord ($t_{1/2}$ = 78 days) and cortex ($t_{1/2}$ = 67 days). Although the concentrations of WVE-004 declined in spinal cord and cortex with time, low

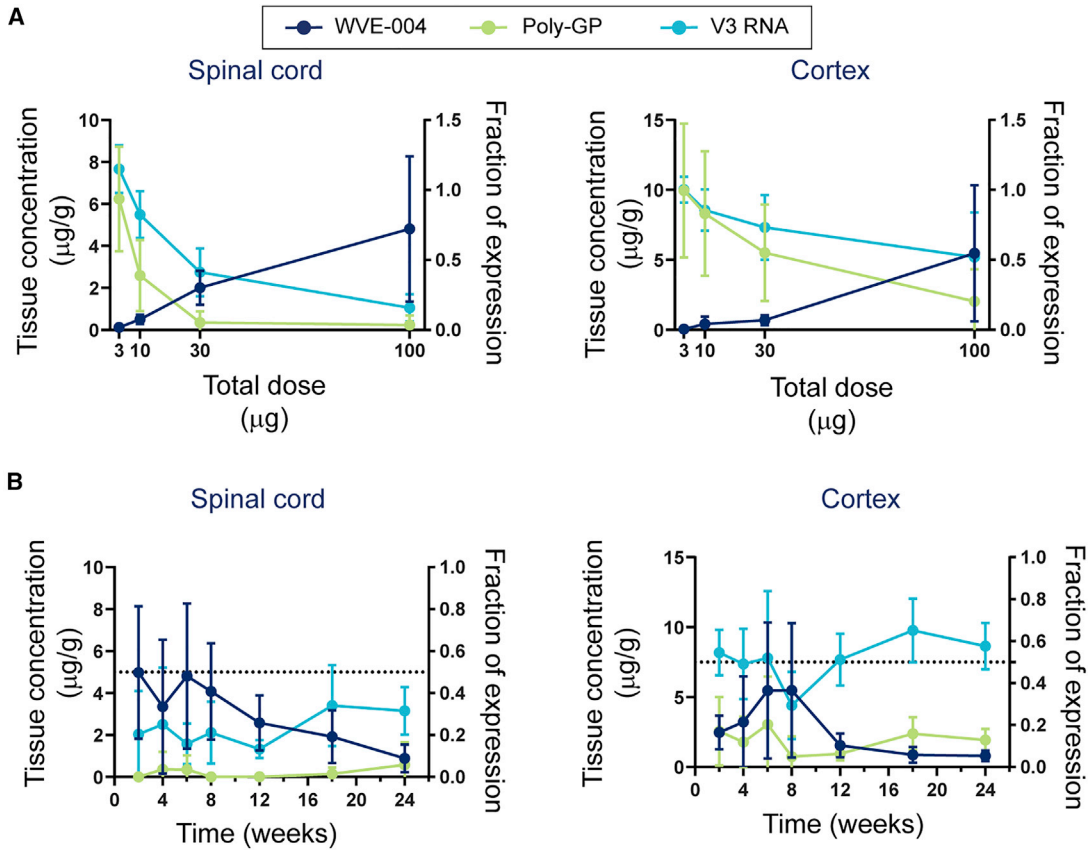

Figure 7. WVE-004 sustains poly-GP reduction and V3 transcript knockdown *in vivo* at low levels of tissue exposure

(A and B) WVE-004 tissue concentrations (navy blue), fraction of V3 transcript expression (light blue), and fraction of poly-GP (green) in (A) C9 BAC mice administered PBS or increasing amounts of WVE-004 and euthanized 6 weeks after the first administration and (B) C9 BAC mice administered PBS or 100 µg total dose WVE-004 and euthanized up to 24 weeks after the first administration. Plots were generated using the same data shown in Figures 4, 5, 6, and S4. Data are shown as mean ± SD. i.c.v., intracerebroventricular; PBS, phosphate-buffered saline; poly-GP, poly-glycine-proline; V, variant.

levels, at or near the IC_{50} concentrations, were sufficient to mediate persistent silencing of V3 transcripts and poly-GP. V3 transcript levels began to rise as tissue exposure decreased but remained at or near the 50% expression level for the duration of the experiments, while poly-GP levels recovered more slowly. These long $t_{1/2}$s (more than 2 months) and the low IC_{50} concentrations are consistent with the durability of the effects we observed on V3 transcripts and poly-GP.

DISCUSSION

We developed an investigational stereopure antisense oligonucleotide, WVE-004, that targets SS1b, a targeting sequence that enables variant-selective silencing of repeat-containing C9orf72 transcripts.[7] We have previously shown that variant-selective stereopure oligonucleotides targeting SS1b lead to the durable depletion of RNA foci and DPRs in C9 BAC mice and protect against glutamate-induced neurotoxicity in human motor neurons expressing the repeat expansion.[7] Herein, we have shown that clinically relevant doses of WVE-004 (a 100 µg dose in mouse corresponds to a human equivalent dose of 24 mg)[52] support durable target engagement and pharmacodynamic effects in ALS- and FTD-relevant tissues. In C9 BAC transgenic mice, WVE-004 produced substantial reductions in V3 expression and poly-GP that are sustained for at least 6 months without disrupting total C9orf72 protein expression. The CNS tissue $t_{1/2}$ of WVE-004 was greater than 2 months, which is consistent with the durability of its effects. Even at later time points, when tissue concentrations of WVE-004 were markedly decreased, knockdown of repeat-containing transcripts and reduction of poly-GP persisted.

In this study, we assessed WVE-004 activity by measuring levels of its direct target, repeat-containing C9orf72 transcripts, as well as a downstream biomarker of activity, poly-GP. These pathogenic repeat-containing transcripts can lead to RNA foci as well as the translation of DPRs that can form aggregates and cause neurotoxicity.[1,37,40,50] Reduction of V3 transcripts have been shown to reduce RNA foci.[7] Consistent with previous studies, when V3 transcript levels decreased, we also observed a corresponding decrease in poly-GP levels.[7,46,50] Poly-GP is present in

the CSF of both symptomatic and asymptomatic *C9orf72*-expansion carriers. Longitudinally collected CSF samples from 33 *C9orf72*-expansion carriers (symptomatic: n = 24, asymptomatic: n = 9) showed no evidence of a significant change in poly-GP levels over time (median: 12.9 months, range: 4.4–22.6 months).[50] This stability, combined with its strong correlation with the knockdown of repeat-containing transcripts, makes poly-GP an important biomarker for potential therapeutics targeting repeat-containing transcripts that enter clinical development. Although poly-GP levels were variable in controls, they remained uniformly low after treatment even after V3 transcript levels started to rise, which is consistent with its production downstream of repeat-containing transcripts, and this kinetic relationship has been observed in other reports.[7,46] While WVE-004 demonstrated substantial activity against repeat-containing C9orf72 transcripts, it did not alter C9orf72 protein levels, avoiding further haploinsufficiency and demonstrating a key benefit of using a variant-selective approach to C9orf72 knockdown, as the partial loss of function of C9orf72 protein is thought to contribute to C9-ALS/FTD.[7,27,33]

We have previously shown that the stereopure oligonucleotide C9orf72-631, which also targets SS1b, outperformed other C9orf72-targeting oligonucleotides that have been reported in the literature.[7] WVE-004's activity profile represents an improvement over C9orf72-631 and all of these previously published molecules. It contains a combination of stereopure PS and PN linkages, which we have previously shown can improve potency, distribution, and durability compared with similar PS-modified antisense oligonucleotides in the CNS.[45] Herein, we reinforce these findings by showing that WVE-004 can lead to sustained reductions in V3 transcripts and poly-GP in the spinal cord and cortex for at least 6 months. To our knowledge, this long-term effect with a relatively low dose is unprecedented in the CNS of mouse models.[53–55]

WVE-004 significantly reduced both V3 transcripts and poly-GP levels in the spinal cord as well as the cortex. This has important implications for ALS, FTD, or mixed phenotype-disease with C9orf72-repeat expansion: despite sharing an underlying genetic mutation, neurodegeneration manifests in different brain regions in each disease.[8,12,18] The results of this study show that WVE-004 has the potential to target the upper and lower motor neurons of the motor cortex and spinal cord affected by ALS as well as to reach cortical neurons of the frontal and temporal cortices affected by FTD. As such, WVE-004 has the potential to address the genetic root cause of both diseases. Notably, this makes WVE-004 the first oligonucleotide to enter clinical trials for the treatment of patients with C9-FTD, as other clinical programs designed to address the *C9orf72*-repeat expansion are only being tested in C9-ALS (ClinicalTrials.gov: NCT03626012 and NCT04288856).

With WVE-004, we report a stereopure antisense oligonucleotide that executes our desired variant-selective mechanism of action against repeat-expanded *C9orf72*. WVE-004 leads to potent, selective, and durable knockdown of pathogenic repeat-containing transcripts and their derivatives while preserving C9orf72 protein in C9 BAC mice. Wave Life Sciences has initiated dosing in the FOCUS-C9 study (ClinicalTrials.gov: NCT04931862), in which WVE-004 is being evaluated for efficacy and safety in patients with C9-ALS/FTD or mixed phenotypes.

MATERIALS AND METHODS

WVE-004

WVE-004 is a stereopure antisense oligonucleotide (5'-ACTCACC CACTCGCCACCGC-3′), containing both PS and PN backbone modifications. WVE-004 contains asymmetric 2′-ribose modifications in its 5' and 3′ ends[7]. It was synthesized as described previously.[56] The NTC used in this work is a stereorandom PS-modified oligonucleotide with the same 2′-ribose modification pattern as WVE-004 (5′-CCTTCCCTGAAGGTTCCUCC-3′).

In vitro experiments

iPSC-derived ALS motor-neuron differentiation

iPSC-derived motor neurons from a patient with C9-ALS were differentiated at BrainXell. Spinal motor neurons were generated from a human ALS iPSC line harboring a *C9orf72* expansion (Target ALS: TALS9-9.3; Rutgers: 150,000,000002; NINDS: ND50000). Directed differentiation was performed as described.[57] Briefly, iPSCs were treated with the small molecules CHIR99021, DMH-1, and SB431542 for 6 days to induce $SOX1^+$ neuroepithelial progenitors (NEPs). The NEPs were split and treated with CHIR99021, DMH-1, SB431542, retinoic acid, and purmorphamine for another 6 days to generate $OLIG2^+$ motor-neuron progenitors (MNPs). These $OLIG2^+$ MNPs were expanded and frozen at the point of early differentiation to motor neurons.

ALS motor-neuron culture and oligonucleotide treatment

ALS motor neurons were treated with an oligonucleotide as previously described.[7] Briefly, cryopreserved motor neurons (5×10^6 cells per vial) were thawed at day 0 on poly-D-lysine-coated 12-well plates. WVE-004 or a NTC was added on day 7 at various concentrations. On day 10, 50 μL of a growth factor cocktail containing 10 ng brain-derived neurotrophic factor (BDNF), 10 ng glial-cell-derived neurotrophic factor (GDNF), and 1 ng transforming growth factor beta 1 (TGF-β1) were added into each well. Cells were harvested on day 14 (7 days post-treatment).

C9orf72 transcript-quantification assays

ALS motor neurons were collected, and total RNA was extracted using Trizol (Invitrogen, Waltham, MA, USA) according to the manufacturer's protocol and quantified as previously described.[7] Taqman probes used were Hs00376619_m1 (FAM) for all transcripts, Hs00948764_m1 (FAM) for V3 transcripts, and Hs02800695_m1 for human *HPRT1* transcripts. Quantitative polymerase chain reaction (qPCR): 3 min at 95°C, 40 cycles of 10 s at 95°C, and 30 s at 60°C. qPCR was performed on a C1000 Touch Thermocycler, and data were analyzed using Bio-Rad CFX Maestro, Microsoft Excel, and GraphPad Prism software.

PBMC experiments

Fresh human PBMCs from three donors (donor 1: 3033038, donor 2: 3033468, and donor 3: 3033043) were from AllCell (cat. no. LP, FR, MNC, 100 M). Human PBMCs were cultured and assayed in IMDM (Life Technologies, Carlsbad, CA, USA, cat. no. 12440-053) supplemented with 10% HI FBS (Life Technologies, cat. no. 10082-147) and 1% penicillin-streptomycin (Pen-Strep; Lonza, Basel, Switzerland, cat. no. 17–602E). The pro-inflammatory potential of WVE-004 was investigated *ex vivo* in multiplex cytokine assays on PBMCs treated with PBS (non-inflammatory control), WVE-004, and ODN 2216 (a pro-inflammatory oligonucleotide).[44] On the same day of cell arrival, cell density and viability were determined by trypan-blue exclusion. Required amounts of cells were spun down at 350 × *g* for 5 min then were resuspended in fresh medium. The final plating density was 4×10^5 cells/150 μL per well. Cells were incubated with PBS, 0.1–30 μM WVE-004, or 1.0 μg/mL ODN 2216 for 24 h at 37°C, 95% humidity, and 5% CO_2 with constant agitation. At the conclusion of treatment, cells were spun down before supernatant was collected. The multiplex cytokine assay was performed following manufacturer's protocol (EMD cat. no. HCYTMAG-60K) with modifications. Fluorescence intensity was read on FLEXMAP3D system (Luminex, Austin, TX, USA). Homogenous cell suspensions (10 μL) were collected and mixed with equal volume of Cell Titer-Glow to determine ATP levels (CellTiter-Glo 2.0, Promega, Madison, WI, USA, cat. no. G9242). Cytokine levels were determined using a 5-parameter nonlinear regression fit.

Animal experiments

Animal compliance

All animal experiments were performed at Biomere (Worcester, MA, USA) in compliance with Biomere's Institutional Animal Care and Use Committee guidelines for care and use of animals.

Mice

The transgenic line Tg(C9orf72_3) line 112 mice (JAX stock no. 023099) used for *in vivo* pharmacological studies has been described in O'Rourke et al.[47] This BAC transgenic line has several tandem copies of the full-length *C9orf72* transgene, with each copy having between 100 and 1,000 repeats. Male and female mice used in this study were 16 to 24 weeks of age at the time of dosing. Subjects were balanced across treatment groups by gender and age.

i.c.v. cannulation surgery

For injections of oligonucleotides into the lateral ventricle, mice were deeply anesthetized under avertin and placed on a rodent stereotaxic apparatus; they were then implanted with a stainless-steel guide cannula in the right lateral ventricle (coordinates: -0.3 mm posterior, +1.0-mm lateral, and -2.2 mm vertically from bregma), which was secured using dental cement. Mice were allowed a 1-week recovery period prior to the injection of compounds.

i.c.v. injections

For the dose-response studies, injection of PBS or 1.5, 5, 15, or 50 μg of oligonucleotide was performed in conscious mice (through the guide cannula) in a volume of 2.5 μL on day 0, which was followed by a second injection of the same concentration and volume on day 7. The same injection procedures were followed for the 8-week and 24-week duration of action studies at the 50 μg oligonucleotide dose.

Necropsy

Euthanasia was performed on day 14, 28, 42, 56, 84, 126, or 168; the mice were euthanized with CO_2 and transcardially perfused with 1× PBS. Brains were rapidly removed from the skull, and the left hemisphere was drop-fixed in 10% formalin and processed for histological analyses. Cortices from the right hemisphere were flash frozen on dry ice and used for biochemical analysis. Spinal cord sections were separated and frozen on dry ice for biochemical analysis.

Tissues processing for transcript analyses by PCR and oligonucleotide quantification by hybridization enzyme-linked immunosorbent assay (ELISA)

Cortex and upper lumbar spinal cord tissues were processed and quantified as previously described.[7] Tissue lysate (25–45 μL) was saved at -80°C in 96-well plates for pharmacokinetic (PK) measurements. The remaining Trizol lysates were used for RNA extraction. The same Taqman probes used for ALS motor neurons were used for qPCR. The following probes were designed to selectively quantify the oligonucleotide used in this study by hybridization ELISA: capture probe, "WV-21522-CAP"/5AmMC12/GCGG + TGGCG + A"; detection probe, "WV-21522-Det": G + TGGG + TG + AGT/3BioTEG/." Samples were read on the Molecular Device, M5 fluorescence channel plate reader: Ex435 nm and Em555 nm. The oligonucleotide in samples was calculated according to standard curve by 4-parameter regression.

ViewRNA *in situ* hybridization (ISH) assay (formalin sections)

Formalin-fixed, paraffin-embedded (FFPE) sections were prepared as previously described.[7] Treated slides were rinsed in 1× PBS with agitation and then treated with QuantiGene ViewRNA miRNA probe sets of DVM1-10834 for WV-004, peptidylprolyl isomerase B (PPiB) (positive control), and/or dihydrodipicolinate reductase (dapB) (negative control) diluted to 12.5 nM in pre-warmed Probe Set Diluent QT (300 μL per section) for 2 h at 40°C. For signal amplification and detection, slides were prepared as previously described.[7] Nucleic acid DNA was counterstained with hematoxylin and/or Hoechst 33342 dye. The slides were mounted with ProLong Gold Antifade mounting medium and covered with a thin glass coverslip. For each hemibrain/spinal cord cross-section, the representative digital images were generated using a Zeiss Axio Observer microscope under bright-field or fluorescent-field illumination. This method was used for assessment after 8 weeks of treatment. We evaluated 4 animals treated with WVE-004 and 4 animals treated with PBS.

ViewRNA ISH assay (OCT embedded sections)

A ViewRNA ISH Tissue 1-Plex Assay was adapted for detection of oligonucleotide *in situ*. Briefly, the spinal cord biopsies were freshly frozen and embedded with OCT compound. After sectioning

(10 μm), the slides were dried for 2 h, fixed in 4% PFA (made in DEPC-PBS) for 30 min at room temperature, rinsed 3 times in PBS, and stored in pre-chilled 70% ethanol overnight at -4°C. The next day, slides were rehydrated in PBS and treated with protease (Protease QF 1:100 in 1× PBS, pre-warmed) at 40°C for 30 min. Slides were rinsed in 1× PBS with agitation and then treated with the QuantiGene ViewRNA miRNA probe set (as described above). For signal amplification and detection, rinsed slides were incubated in working PreAmp1 QF solution diluted at 1:200 in pre-warmed Amplifier Diluent QF for 30 min at 40°C, rinsed in wash buffer with agitation, followed by incubation in working Amp1 QF solution (diluted at 1:200 in pre-warmed Amplifier Diluent QF) for 20 min at 40°C, and rinsed in wash buffer with agitation. We incubated the slides in Label Probe-AP working solution (diluted 1:1,000 in Label Probe Diluent QF) for 20 min at 40°C and rinsed in wash buffer with agitation. AP-Enhancer Solution was added for 5 min at room temperature before adding Fast Red Substrate and incubation for 30 min at 40°C to develop red color deposit. Slides were counter-stained and mounted, and images were captured as described above. This method was used for animals treated for 24 weeks. We evaluated 4 animals treated with WVE-004 and 3 animals treated with PBS.

Poly-GP quantification using the meso scale discovery (MSD) platform

Brain and spinal cord samples were prepared as previously described.[7] Samples were read in the MSD QuickPlex SQ 120 plate reader. A standard curve of recombinant purified GST-GP32 was prepared in a matrix of wild-type (WT) mouse cortex or spinal cord homogenate normalized to the same concentration as the samples. A 4-parameter logistic fit line for the standard curve was used to interpolate the concentration of poly-GP in ng/mg of tissue for the samples.

C9orf72 protein analysis using capillary western immunoassay (WES)

C9orf72 quantitation was performed on a WES system, according to the manufacturer's instructions, using a 12–230 kDa separation module, the anti-rabbit detection module, and the anti-mouse detection module. The following antibodies were used: mouse anti-C9orf72 GT779 (1:100, GeneTex, Irvine, CA, USA), rabbit anti-HPRT (1:250 in antibody diluent, Novus Biologicals, Littleton, CO, USA), and HRP-conjugated secondary antibodies (ready to use anti-mouse combined with ready to use anti-rabbit in 1:1 ratio). The following instrument default settings were used: stacking and separation at 475 V for 30 min, blocking reagent for 5 min, primary and secondary antibody both for 30 min, and luminol/peroxide chemiluminescence detection for ∼15 min. The calculated concentrations were analyzed by dividing the area under the curve (AUC) of the C9orf72 peak by the AUC of the HPRT peak. Then, the concentrations from the PBS-treated group of animals were averaged, and all data points were divided by this value.

In vivo IC_{50} calculation

The IC_{50} values were determined from PK and PD data (dose-response and duration study results were pooled) using a population nonlinear mixed-effect (NMLE) modeling approach. Estimation was done by executing the inhibition-limited indirect PK/PD model with fixed E_0 (the effect at 0 drug concentration) and I_{max} (maximum inhibition) values.

Statistical analyses

Unless otherwise indicated, data were analyzed by a one-way or two-way analysis of variance followed by post-hoc analyses for multiple comparisons with Dunnett's or Sidak's multiple comparison test using GraphPad Prism software.

We will distribute materials and protocols upon request from qualified researchers pursuant to a Material Transfer Agreement and subject to payment for maintenance and transport of materials.

SUPPLEMENTAL INFORMATION

Supplemental information can be found online at https://doi.org/10.1016/j.omtn.2022.04.007.

ACKNOWLEDGMENTS

The authors would like to thank Tomomi Kawamoto, Megan Cannon, and Jake Metterville from Wave Life Sciences for the execution of *in vivo* studies. We thank Judy Bloom, PhD (Chameleon Communications International with funding from Wave Life Sciences) and Amy Donner (Wave Life Sciences) for assistance in the preparation of this report. This study was funded by Wave Life Sciences.

AUTHOR CONTRIBUTIONS

Conceptualization, Y.L., E.D., N.I., and C.V.; methodology, Y.L., A.A., X.L., H.Y., and S.M.; formal analysis, Y.L., N.I., A.B., X.S.H., X.L., and S.L.; investigation, Y.L., A.A., N.I., Y.Y., F.L., S.P., S.M., E.P.-E., and K.T.; writing – review & editing, Y.L., A.A., N.I., Y.Y., H.Y., F.L., A.B., X.S.H., X.L., S.L., S.P., S.M., E.P.-E., K.T., E.D., and C.V.; data curation, Y.L., N.I., X.L., S.L., and H.Y.; visualization, Y.L., F.L., A.B., and X.S.H.; supervision, Y.L., N.I., H.Y., X.S.H., E.D., S.L., and C.V.

DECLARATION OF INTERESTS

Y.L., A.A., N.I., Y.Y., H.Y., F.L., A.B., X.S.H., X.L., S.L., S.P., S.M., E.P.-E., K.T., E.D., and C.V. were employees of Wave Life Sciences during the completion of this work. Y.L., A.A., N.I., S.M., and C.V. have patents associated with this work.

REFERENCES

1. DeJesus-Hernandez, M., Mackenzie, I.R., Boeve, B.F., Boxer, A.L., Baker, M., Rutherford, N.J., Nicholson, A.M., Finch, N.A., Flynn, H., Adamson, J., et al. (2011). Expanded GGGGCC hexanucleotide repeat in noncoding region of C9ORF72 causes chromosome 9p-linked FTD and ALS. Neuron *72*, 245–256. https://doi.org/10.1016/j.neuron.2011.09.011.

2. Renton, A.E., Majounie, E., Waite, A., Simon-Sanchez, J., Rollinson, S., Gibbs, J.R., Schymick, J.C., Laaksovirta, H., van Swieten, J.C., Myllykangas, L., et al. (2011). A hexanucleotide repeat expansion in C9ORF72 is the cause of chromosome 9p21-linked ALS-FTD. Neuron *72*, 257–268. https://doi.org/10.1016/j.neuron.2011.09.010.

3. Turner, M.R., Al-Chalabi, A., Chio, A., Hardiman, O., Kiernan, M.C., Rohrer, J.D., Rowe, J., Seeley, W., and Talbot, K. (2017). Genetic screening in sporadic ALS and

FTD. J. Neurol. Neurosurg. Psychiatry *88*, 1042–1044. https://doi.org/10.1136/jnnp-2017-315995.

4. Boeve, B.F., Boylan, K.B., Graff-Radford, N.R., DeJesus-Hernandez, M., Knopman, D.S., Pedraza, O., Vemuri, P., Jones, D., Lowe, V., Murray, M.E., et al. (2012). Characterization of frontotemporal dementia and/or amyotrophic lateral sclerosis associated with the GGGGCC repeat expansion in C9ORF72. Brain *135*, 765–783. https://doi.org/10.1093/brain/aws004.

5. Mahoney, C.J., Beck, J., Rohrer, J.D., Lashley, T., Mok, K., Shakespeare, T., Yeatman, T., Warrington, E.K., Schott, J.M., Fox, N.C., et al. (2012). Frontotemporal dementia with the C9ORF72 hexanucleotide repeat expansion: clinical, neuroanatomical and neuropathological features. Brain *135*, 736–750. https://doi.org/10.1093/brain/awr361.

6. Byrne, S., Elamin, M., Bede, P., Shatunov, A., Walsh, C., Corr, B., Heverin, M., Jordan, N., Kenna, K., Lynch, C., et al. (2012). Cognitive and clinical characteristics of patients with amyotrophic lateral sclerosis carrying a C9orf72 repeat expansion: a population-based cohort study. Lancet Neurol. *11*, 232–240. https://doi.org/10.1016/s1474-4422(12)70014-5.

7. Liu, Y., Dodart, J.C., Tran, H., Berkovitch, S., Braun, M., Byrne, M., Durbin, A.F., Hu, X.S., Iwamoto, N., Jang, H.G., et al. (2021). Variant-selective stereopure oligonucleotides protect against pathologies associated with C9orf72-repeat expansion in preclinical models. Nat. Commun. *12*, 847. https://doi.org/10.1038/s41467-021-21112-8.

8. Umoh, M.E., Dammer, E.B., Dai, J., Duong, D.M., Lah, J.J., Levey, A.I., Gearing, M., Glass, J.D., and Seyfried, N.T. (2018). A proteomic network approach across the ALS-FTD disease spectrum resolves clinical phenotypes and genetic vulnerability in human brain. EMBO Mol. Med. *10*, 48–62. https://doi.org/10.15252/emmm.201708202.

9. Strong, M.J., Abrahams, S., Goldstein, L.H., Woolley, S., McLaughlin, P., Snowden, J., Mioshi, E., Roberts-South, A., Benatar, M., HortobáGyi, T., et al. (2017). Amyotrophic lateral sclerosis - frontotemporal spectrum disorder (ALS-FTSD): revised diagnostic criteria. Amyotroph. Lateral Scler. Frontotemporal Degener *18*, 153–174. https://doi.org/10.1080/21678421.2016.1267768.

10. Barker, H.V., Niblock, M., Lee, Y.B., Shaw, C.E., and Gallo, J.M. (2017). RNA misprocessing in C9orf72-linked neurodegeneration. Front. Cell Neurosci *11*, 195. https://doi.org/10.3389/fncel.2017.00195.

11. Chiò, A., Restagno, G., Brunetti, M., Ossola, I., Calvo, A., Canosa, A., Moglia, C., Floris, G., Tacconi, P., Marrosu, F., et al.; the SARDINIALS Consortium (2012). ALS/FTD phenotype in two Sardinian families carrying both C9ORF72 and TARDBP mutations. J. Neurol. Neurosurg. Psychiatry *83*, 730–733. https://doi.org/10.1136/jnnp-2012-302219.

12. Ling, S.C., Polymenidou, M., and Cleveland, D.W. (2013). Converging mechanisms in ALS and FTD: disrupted RNA and protein homeostasis. Neuron *79*, 416–438. https://doi.org/10.1016/j.neuron.2013.07.033.

13. Majounie, E., Renton, A.E., Mok, K., Dopper, E.G., Waite, A., Rollinson, S., Chio, A., Restagno, G., Nicolaou, N., Simon-Sanchez, J., et al. (2012). Frequency of the C9orf72 hexanucleotide repeat expansion in patients with amyotrophic lateral sclerosis and frontotemporal dementia: a cross-sectional study. Lancet Neurol. *11*, 323–330. https://doi.org/10.1016/s1474-4422(12)70043-1.

14. Mehta, P., Kaye, W., Raymond, J., Punjani, R., Larson, T., Cohen, J., Muravov, O., and Horton, K. (2018). Prevalence of amyotrophic lateral sclerosis - United States, 2015. MMWR Morb Mortal Wkly Rep. *67*, 1285–1289. https://doi.org/10.15585/mmwr.mm6746a1.

15. Chen, S., Sayana, P., Zhang, X., and Le, W. (2013). Genetics of amyotrophic lateral sclerosis: an update. Mol. Neurodegeneration *8*, 28. https://doi.org/10.1186/1750-1326-8-28.

16. Brown, C.A., Lally, C., Kupelian, V., and Flanders, W.D. (2021). Estimated prevalence and incidence of amyotrophic lateral sclerosis and SOD1 and C9orf72 genetic variants. Neuroepidemiology *55*, 342–353. https://doi.org/10.1159/000516752.

17. Cammack, A.J., Atassi, N., Hyman, T., van den Berg, L.H., Harms, M., Baloh, R.H., Brown, R.H., van Es, M.A., Veldink, J.H., de Vries, B.S., et al.; Alzheimer's Disease Neuroimaging Initiative (2019). Prospective natural history study of C9orf72 ALS clinical characteristics and biomarkers. Neurology *93*, e1605–e1617. https://doi.org/10.1212/wnl.0000000000008359.

18. Balendra, R., and Isaacs, A.M. (2018). C9orf72-mediated ALS and FTD: multiple pathways to disease. Nat. Rev. Neurol. *14*, 544–558. https://doi.org/10.1038/s41582-018-0047-2.

19. Onyike, C.U., and Diehl-Schmid, J. (2013). The epidemiology of frontotemporal dementia. Int. Rev. Psychiatry *25*, 130–137. https://doi.org/10.3109/09540261.2013.776523.

20. Moore, K.M., Nicholas, J., Grossman, M., McMillan, C.T., Irwin, D.J., Massimo, L., Van Deerlin, V.M., Warren, J.D., Fox, N.C., Rossor, M.N., et al. (2020). Age at symptom onset and death and disease duration in genetic frontotemporal dementia: an international retrospective cohort study. Lancet Neurol. *19*, 145–156. https://doi.org/10.1016/s1474-4422(19)30394-1.

21. Stevens, M., van Duijn, C.M., Kamphorst, W., de Knijff, P., Heutink, P., van Gool, W.A., Scheltens, P., Ravid, R., Oostra, B.A., Niermeijer, M.F., and van Swieten, J.C. (1998). Familial aggregation in frontotemporal dementia. Neurology *50*, 1541–1545. https://doi.org/10.1212/wnl.50.6.1541.

22. Heuer, H.W., Wang, P., Rascovsky, K., Wolf, A., Appleby, B., Bove, J., Bordelon, Y., Brannelly, P., Brushaber, D.E., Caso, C., et al.; on behalf of the ARTFL and LEFFTDS consortia (2020). Comparison of sporadic and familial behavioral variant frontotemporal dementia (FTD) in a North American cohort. Alzheimers Dement *16*, 60–70. https://doi.org/10.1002/alz.12046.

23. Snowden, J.S., Rollinson, S., Thompson, J.C., Harris, J.M., Stopford, C.L., Richardson, A.M.T., Jones, M., Gerhard, A., Davidson, Y.S., Robinson, A., et al. (2012). Distinct clinical and pathological characteristics of frontotemporal dementia associated with C9ORF72 mutations. Brain *135*, 693–708. https://doi.org/10.1093/brain/awr355.

24. Chiò, A., Moglia, C., Canosa, A., Manera, U., Vasta, R., Brunetti, M., Barberis, M., Corrado, L., D'Alfonso, S., Bersano, E., et al. (2019). Cognitive impairment across ALS clinical stages in a population-based cohort. Neurology *93*, e984–e994. https://doi.org/10.1212/wnl.0000000000008063.

25. (2017). Safety and efficacy of edaravone in well defined patients with amyotrophic lateral sclerosis: a randomised, double-blind, placebo-controlled trial. Lancet Neurol. *16*, 505–512. https://doi.org/10.1016/s1474-4422(17)30115-1.

26. Fang, T., Al Khleifat, A., Meurgey, J.H., Jones, A., Leigh, P.N., Bensimon, G., and Al-Chalabi, A. (2018). Stage at which riluzole treatment prolongs survival in patients with amyotrophic lateral sclerosis: a retrospective analysis of data from a dose-ranging study. Lancet Neurol. *17*, 416–422. https://doi.org/10.1016/s1474-4422(18)30054-1.

27. Aoki, Y., Manzano, R., Lee, Y., Dafinca, R., Aoki, M., Douglas, A.G.L., Varela, M.A., Sathyaprakash, C., Scaber, J., Barbagallo, P., et al. (2017). C9orf72 and RAB7L1 regulate vesicle trafficking in amyotrophic lateral sclerosis and frontotemporal dementia. Brain *140*, 887–897. https://doi.org/10.1093/brain/awx024.

28. Farg, M.A., Sundaramoorthy, V., Sultana, J.M., Yang, S., Atkinson, R.A., Levina, V., Halloran, M.A., Gleeson, P.A., Blair, I.P., Soo, K.Y., et al. (2014). C9ORF72, implicated in amytrophic lateral sclerosis and frontotemporal dementia, regulates endosomal trafficking. Hum. Mol. Genet. *23*, 3579–3595. https://doi.org/10.1093/hmg/ddu068.

29. Braems, E., Swinnen, B., and Van Den Bosch, L. (2020). C9orf72 loss-of-function: a trivial, stand-alone or additive mechanism in C9 ALS/FTD? Acta Neuropathol. *140*, 625–643. https://doi.org/10.1007/s00401-020-02214-x.

30. Jiang, J., and Ravits, J. (2019). Pathogenic mechanisms and therapy development for C9orf72 amyotrophic lateral sclerosis/frontotemporal dementia. Neurotherapeutics *16*, 1115–1132. https://doi.org/10.1007/s13311-019-00797-2.

31. Lagier-Tourenne, C., Baughn, M., Rigo, F., Sun, S., Liu, P., Li, H.R., Jiang, J., Watt, A.T., Chun, S., Katz, M., et al. (2013). Targeted degradation of sense and antisense C9orf72 RNA foci as therapy for ALS and frontotemporal degeneration. Proc. Natl. Acad. Sci. U S A. *110*, E4530–E4539. https://doi.org/10.1073/pnas.1318835110.

32. Swinnen, B., Robberecht, W., and Van Den Bosch, L. (2020). RNA toxicity in non-coding repeat expansion disorders. Embo j *39*, e101112. https://doi.org/10.15252/embj.2018101112.

33. Shi, Y., Lin, S., Staats, K.A., Li, Y., Chang, W.H., Hung, S.T., Hendricks, E., Linares, G.R., Wang, Y., Son, E.Y., et al. (2018). Haploinsufficiency leads to neurodegeneration in C9ORF72 ALS/FTD human induced motor neurons. Nat. Med. *24*, 313–325. https://doi.org/10.1038/nm.4490.

34. O'Rourke, J.G., Bogdanik, L., Yanez, A., Lall, D., Wolf, A.J., Muhammad, A.K.M.G., Ho, R., Carmona, S., Vit, J.P., Zarrow, J., et al. (2016). C9orf72 is required for proper macrophage and microglial function in mice. Science *351*, 1324–1329. https://doi.org/10.1126/science.aaf1064.

35. Zhu, Q., Jiang, J., Gendron, T.F., McAlonis-Downes, M., Jiang, L., Taylor, A., Diaz Garcia, S., Ghosh Dastidar, S., Rodriguez, M.J., King, P., et al. (2020). Reduced C9ORF72 function exacerbates gain of toxicity from ALS/FTD-causing repeat expansion in C9orf72. Nat. Neurosci. *23*, 615–624. https://doi.org/10.1038/s41593-020-0619-5.

36. Yang, Q., Jiao, B., and Shen, L. (2020). The development of C9orf72-related amyotrophic lateral sclerosis and frontotemporal dementia disorders. Front. Genet. *11*, 562758. https://doi.org/10.3389/fgene.2020.562758.

37. Boivin, M., Pfister, V., Gaucherot, A., Ruffenach, F., Negroni, L., Sellier, C., and Charlet-Berguerand, N. (2020). Reduced autophagy upon C9ORF72 loss synergizes with dipeptide repeat protein toxicity in G4C2 repeat expansion disorders. EMBO J. *39*, e100574. https://doi.org/10.15252/embj.2018100574.

38. Gendron, T.F., Bieniek, K.F., Zhang, Y.J., Jansen-West, K., Ash, P.E.A., Caulfield, T., Daughrity, L., Dunmore, J.H., Castanedes-Casey, M., Chew, J., et al. (2013). Antisense transcripts of the expanded C9ORF72 hexanucleotide repeat form nuclear RNA foci and undergo repeat-associated non-ATG translation in c9FTD/ALS. Acta Neuropathol. *126*, 829–844. https://doi.org/10.1007/s00401-013-1192-8.

39. Zu, T., Liu, Y., Banez-Coronel, M., Reid, T., Pletnikova, O., Lewis, J., Miller, T.M., Harms, M.B., Falchook, A.E., Subramony, S.H., et al. (2013). RAN proteins and RNA foci from antisense transcripts in C9ORF72 ALS and frontotemporal dementia. Proc. Natl. Acad. Sci. U S A *110*, E4968–E4977. https://doi.org/10.1073/pnas.1315438110.

40. Wen, X., Tan, W., Westergard, T., Krishnamurthy, K., Markandaiah, S.S., Shi, Y., Lin, S., Shneider, N.A., Monaghan, J., Pandey, U.B., et al. (2014). Antisense proline-arginine RAN dipeptides linked to C9ORF72-ALS/FTD form toxic nuclear aggregates that initiate in vitro and in vivo neuronal death. Neuron *84*, 1213–1225. https://doi.org/10.1016/j.neuron.2014.12.010.

41. Sonobe, Y., Ghadge, G., Masaki, K., Sendoel, A., Fuchs, E., and Roos, R.P. (2018). Translation of dipeptide repeat proteins from the C9ORF72 expanded repeat is associated with cellular stress. Neurobiol. Dis. *116*, 155–165. https://doi.org/10.1016/j.nbd.2018.05.009.

42. Abo-Rady, M., Kalmbach, N., Pal, A., Schludi, C., Janosch, A., Richter, T., Freitag, P., Bickle, M., Kahlert, A.K., Petri, S., et al. (2020). Knocking out C9ORF72 exacerbates axonal trafficking defects associated with hexanucleotide repeat expansion and reduces levels of heat shock proteins. Stem Cel. Rep. *14*, 390–405. https://doi.org/10.1016/j.stemcr.2020.01.010.

43. Donnelly, C.J., Zhang, P.W., Pham, J.T., Haeusler, A.R., Mistry, N.A., Vidensky, S., Daley, E.L., Poth, E.M., Hoover, B., Fines, D.M., et al. (2013). RNA toxicity from the ALS/FTD C9ORF72 expansion is mitigated by antisense intervention. Neuron *80*, 415–428. https://doi.org/10.1016/j.neuron.2013.10.015.

44. Mortezagholi, S., Babaloo, Z., Rahimzadeh, P., Namdari, H., Ghaedi, M., Gharibdoost, F., Mirzaei, R., Bidad, K., and Salehi, E. (2017). Evaluation of TLR9 expression on PBMCs and CpG ODN-TLR9 ligation on IFN-α production in SLE patients. Immunopharmacol Immunotoxicol *39*, 11–18. https://doi.org/10.1080/08923973.2016.1263859.

45. Kandasamy, P., Liu, Y., Aduda, V., Akare, S., Alam, R., Andreucci, A., Boulay, D., Bowman, K., Byrne, M., Cannon, M., et al. (2022). Impact of guanidine-containing backbone linkages on stereopure antisense oligonucleotides in the CNS. Nucleic Acids Res. *2*, gkac037. https://doi.org/10.1093/nar/gkac037.

46. Jiang, J., Zhu, Q., Gendron, T.F., Saberi, S., McAlonis-Downes, M., Seelman, A., Stauffer, J.E., Jafar-Nejad, P., Drenner, K., Schulte, D., et al. (2016). Gain of toxicity from ALS/FTD-Linked repeat expansions in C9ORF72 is alleviated by antisense oligonucleotides targeting GGGGCC-containing RNAs. Neuron *90*, 535–550. https://doi.org/10.1016/j.neuron.2016.04.006.

47. O'Rourke, J., Bell, S., Carmona, S., Simpkinson, M., Lall, D., Wu, K., Daughrity, L., Dickson, D., Harms, M., Petrucelli, L., et al. (2015). C9orf72 BAC transgenic mice display typical pathologic features of ALS/FTD. Neuron *88*, 892–901. https://doi.org/10.1016/j.neuron.2015.10.027.

48. Liu, Y., Pattamatta, A., Zu, T., Reid, T., Bardhi, O., Borchelt, D.R., Yachnis, A.T., and Ranum, L.P. (2016). C9orf72 BAC mouse model with motor deficits and neurodegenerative features of ALS/FTD. Neuron *90*, 521–534. https://doi.org/10.1016/j.neuron.2016.04.005.

49. Peters, O.M., Cabrera, G.T., Tran, H., Gendron, T.F., McKeon, J.E., Metterville, J., Weiss, A., Wightman, N., Salameh, J., Kim, J., et al. (2015). Human C9ORF72 hexanucleotide expansion reproduces RNA foci and dipeptide repeat proteins but not neurodegeneration in BAC transgenic mice. Neuron *88*, 902–909. https://doi.org/10.1016/j.neuron.2015.11.018.

50. Gendron, T.F., Chew, J., Stankowski, J.N., Hayes, L.R., Zhang, Y.J., Prudencio, M., Carlomagno, Y., Daughrity, L.M., Jansen-West, K., Perkerson, E.A., et al. (2017). Poly(GP) proteins are a useful pharmacodynamic marker for C9ORF72-associated amyotrophic lateral sclerosis. Sci. Transl Med. *9*, eaai7866. https://doi.org/10.1126/scitranslmed.aai7866.

51. Su, Z., Zhang, Y., Gendron, T.F., Bauer, P.O., Chew, J., Yang, W.Y., Fostvedt, E., Jansen-West, K., Belzil, V.V., Desaro, P., et al. (2014). Discovery of a biomarker and lead small molecules to target r(GGGGCC)-associated defects in c9FTD/ALS. Neuron *83*, 1043–1050. https://doi.org/10.1016/j.neuron.2014.07.041.

52. Nair, A.B., and Jacob, S. (2016). A simple practice guide for dose conversion between animals and human. J. Basic Clin. Pharm. *7*, 27–31. https://doi.org/10.4103/0976-0105.177703.

53. Zhao, H.T., John, N., Delic, V., Ikeda-Lee, K., Kim, A., Weihofen, A., Swayze, E.E., Kordasiewicz, H.B., West, A.B., and Volpicelli-Daley, L.A. (2017). LRRK2 antisense oligonucleotides ameliorate α-synuclein inclusion formation in a Parkinson's disease mouse model. Mol. Ther. Nucleic Acids *8*, 508–519. https://doi.org/10.1016/j.omtn.2017.08.002.

54. Elitt, M.S., Barbar, L., Shick, H.E., Powers, B.E., Maeno-Hikichi, Y., Madhavan, M., Allan, K.C., Nawash, B.S., Gevorgyan, A.S., Hung, S., et al. (2020). Suppression of proteolipid protein rescues Pelizaeus-Merzbacher disease. Nature *585*, 397–403. https://doi.org/10.1038/s41586-020-2494-3.

55. Raymond, G.J., Zhao, H.T., Race, B., Raymond, L.D., Williams, K., Swayze, E.E., Graffam, S., Le, J., Caron, T., Stathopoulos, J., et al. (2019). Antisense oligonucleotides extend survival of prion-infected mice. JCI insight *4*, e131175. https://doi.org/10.1172/jci.insight.131175.

56. Kandasamy, P., McClorey, G., Shimizu, M., Kothari, N., Alam, R., Iwamoto, N., Kumarasamy, J., Bommineni, G.R., Bezigian, A., Chivatakarn, O., et al. (2022). Control of backbone chemistry and chirality boost oligonucleotide splice switching activity. Nucleic Acids Res. *21*, gkac018. https://doi.org/10.1093/nar/gkac018.

57. Du, Z.W., Chen, H., Liu, H., Lu, J., Qian, K., Huang, C.L., Zhong, X., Fan, F., and Zhang, S.C. (2015). Generation and expansion of highly pure motor neuron progenitors from human pluripotent stem cells. Nat. Commun. *6*, 6626. https://doi.org/10.1038/ncomms7626.